ELSEVIER

On the role of dynamical synapses in coincidence detection

Lovorka Pantic*, Joaquín J. Torres, Hilbert J. Kappen

*Department of Medical Physics and Biophysics, University of Nijmegen, Geert Grooteplein 21,
CPK1 231 NL, 6525 EZ Nijmegen, Netherlands*

Abstract

In a number of recent experimental studies it has been reported that synaptic transmission is activity-dependent process. In this paper we study whether and how the synaptic plasticity, in particular, short-term depression affects coincidence detection. We explore the responses of a neuron to massive input of Poisson distributed spike trains containing a signal of coincident presynaptic spikes. Our numerical and analytical results indicate that depressed (dynamic) synapses are capable of coincidence detection over a larger frequency range than non-depressed (static) synapses. The conclusion is not particularly dependent on the neuron model and holds for both integrate-and-fire and Hodgkin–Huxley models. © 2001 Elsevier Science B.V. All rights reserved.

PACS: 87.17.Aa; 87.18.Sn; 87.19.La

Keywords: Short term depression; Coincidence detection; Dynamic synapses

1. Introduction

Recent experimental studies of cortical neurons have shown that the postsynaptic potential is a dynamical quantity that depends on the presynaptic input history [1,4,7,8,11,13]. After an excitatory postsynaptic potential (EPSP) the synapse needs to recover before it restores to its original strength. Thus, the EPSP amplitude tends to decrease with the input frequency of presynaptic spike trains. This behavior is known as short-term synaptic depression and it is well captured by the *dynamical* model of synapses introduced in [13]. Much theoretical work on neural networks has been

---

*Corresponding author. Tel.: +31-24-3614230; fax: +31-24-3541435.
E-mail address: lovorka@mbfys.kun.nl (L. Pantic).

done with the use of static model which does not provide such a frequency dependence. The fact that synaptic strength is a function of neural activity, greatly affects our traditional view of neural processing such as recurrent excitation, cell assemblies and memory as attractors.

In this paper we study the responses of a single neuron when Poisson spike trains stimulate its N synapses. A subset of $M < N$ synapses receives fully correlated inputs (i.e. identical Poisson spike trains) constituting a "signal" term while the remaining $N - M$ synapses, stimulated by uncorrelated spike trains, act like a "noise" term in the synaptic input. We have analyzed whether and how coincidence detection of the signal depends on the type of a synapse, i.e. depressed (dynamic) or non-depressed (static). Motivation for this analysis arises from physiological evidence indicating that precise temporal correlation among neurons encodes various stimulus features [2,3,12,15]. Coincidence detection represents an obvious mechanism to exploit this fact. We present numerical and analytical results that show the detection abilities of an integrate-and-fire (IF) [14] neuron with parameters typical for pyramidal cells. We conclude that the depressed synapses enable the neuron to detect the signal over a bigger range of input frequencies. The conclusion appears to be model independent and also is valid for the Hodgkin–Huxley (HH) [5] neuron.

2. Model

We consider a single neuron that receives inputs from N *excitatory* synapses. All inputs are modeled as Poisson processes with the same mean firing rate f. According to the model introduced in [13], each depressed synapse i is characterized by its amount of resources distributed in recovered (x_i), active (y_i) and inactive (z_i) state. Transitions between these states are governed by first-order dynamics with time constants for inactivation ($\tau_{in} = 3$ ms) and recovery ($\tau_{rec} = 800$ ms). The postsynaptic current is proportional to the amount of resources in the active state, that is, $I_{syn}^i(t) = A_{SE} y_i(t)$, where the parameter A_{SE} represents an absolute strength of the synapse. A natural and simple way to define *static* (non-depressed) synapse from this model is to consider $x(t) = 1 \, \forall t.$[1] Under this assumption it can be shown that the amplitude of the (static) postsynaptic current does not depend on the frequency of the input train. For both descriptions, dynamic or static, the total synaptic current is given by $I_{syn} = \sum_{i=1}^{N} I_{syn}^i$.

We use a standard IF neuron, whose membrane potential satisfies

$$\tau_m \, dV/dt = -V + R_{in} I_{syn}. \tag{1}$$

Parameters have been taken typical for cortical cells [6,13], i.e. an input resistance $R_{in} = 100 \, M\Omega$ and membrane time constant $\tau_m = 15$ ms. We have considered the threshold for firing $V_{th} = 13$ mV above the resting potential $V_{rest} = 0$. Every time that EPSP reaches V_{th}, an action potential is generated and the membrane potential is

---

[1] An equivalent definition is to consider $\tau_{rec} \to 0$.

reset to zero. We choose an absolute refractory period $\tau_{ref} = 5$ ms. For dynamic synapse, we use $A_{SE} = 42.5$ pA to ensure firing at $V_{th} = 13$ mV with $N = 1000$ excitatory synapses. For static synapse we have adjusted $A_{SE} = 8.5$ pA to obtain the same output rate at 10 Hz for both synaptic descriptions.

3. Results

We have analyzed the responses of the neuron with $N = 1000$ and $M = 200$.[2] To find the parameter regions of good detection we have varied the frequency and threshold within the ranges 1–90 Hz and 0.003–0.033 V, respectively. For each frequency and threshold, the following quantities have been computed: (a) the total number of correlated inputs (N_{inputs}), and (b) the number of output spikes occurring immediately (within the time window of 5 ms) after the correlated inputs, that is, *hits* (N_{hits}), (c) the number of output spikes occurring independently of correlated inputs, that is, *false-hits* (N_{falses}), and (d) the number of output spikes that did not appear due to subthreshold level of voltage and due to membrane's non-excitability during an absolute refractory period, i.e. *failures* ($N_{failures}$). We have defined the coincidence detection error as

$$\text{Error} = \frac{N_{falses} + N_{failures}}{N_{inputs}}. \tag{2}$$

Fig. 1(A) (top) shows the coincidence detection error as a function of the frequency and threshold, computed numerically for the neuron with either dynamic or static synapses. For static synapse it appears that no matter how low or high the threshold value is, the frequency window is no wider than about 10 Hz. For dynamic synapse, however, there is an optimal threshold for which good coincidence detection is observed for any frequency between 0 and 50 Hz.

To reproduce these phase diagrams analytically, we assume that the input consists of a constant current due to noise (we can neglect fluctuations in the large $N - M$ limit) plus a deterministic signal current pulse. From the definition of N_{falses} and the IF model we obtain

$$N_{falses} = \frac{\theta(V_{noise} - V_{th})N_{inputs}}{f[\tau_{ref} + \tau_m V_{th}/V_{noise}]}, \tag{3}$$

where $V_{noise} \equiv R_{in}I_{noise} = \{(N - M)f\tau_{in}U_{SE}\}(1 + f\tau_{rec}U_{SE})^{-1}R_{in}A_{SE}$, $\theta(x)$ is the step function, and I_{noise} is the mean EPSC due to "noise" [13]. On the other hand, $N_{failures}$ increases every time the voltage produced by "signal" plus "noise" does not reach the threshold. Thus, when N_{inputs} arrive

$$N_{failures} = [1 - \theta(V_{noise} + V_{signal} - V_{th})]N_{inputs} \tag{4}$$

---

[2] Here, it is worth mentioning that the minimal percentage for detection is related to the membrane time constant τ_m: smaller τ_m allows smaller percentage of coincident spikes.
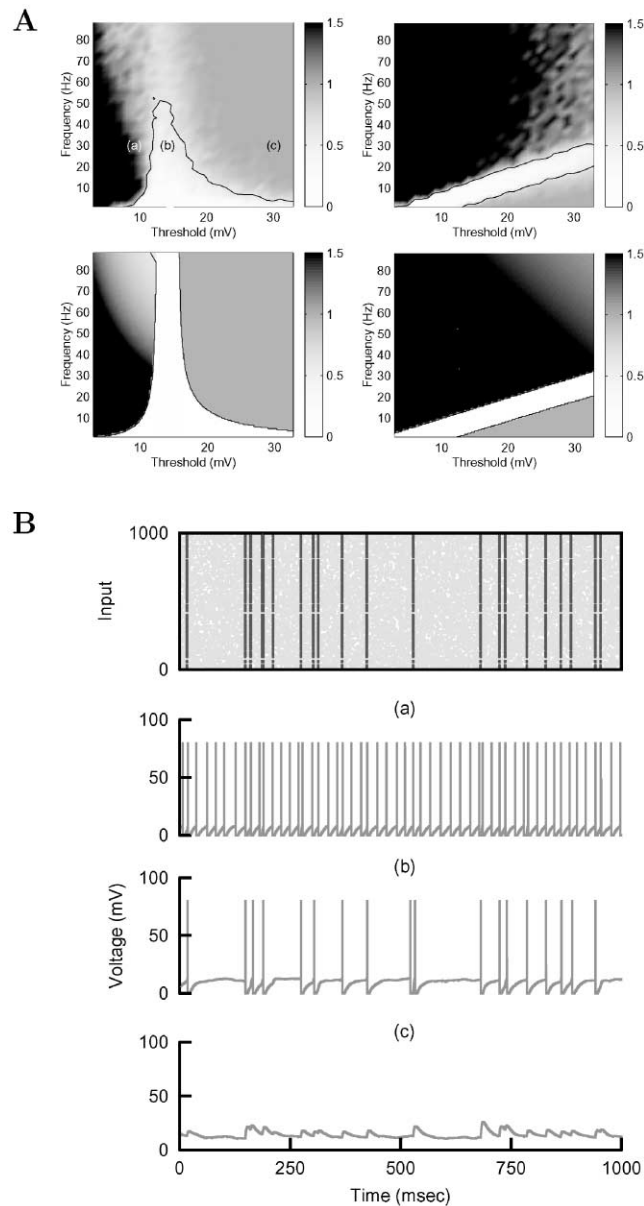
A

B

Fig. 1. Detection abilities of the IF neuron. (A) (Top) the regions of detection found numerically for the IF neuron with either dynamic (left) or static (right) synapses, respectively, where 20% of the synapses receive correlated spike trains. The light area lying inside the contour is a region for which the neuron is able to detect the signal with less than 60% of errors. The black and gray regions are the zones with high percentage of errors. Color coding is identical in both figures. (Bottom) Figures represent the analytical result (Eq. (3)–(5)) showing good agreement with numerical results. (B) The subfigures (a), (b), (c) show the typical behavior occurring in areas marked with (a), (b), (c) in the panel (A). From top to bottom, they represent the synaptic input at 30 Hz, membrane potential for the threshold values of 8 mV (false-hits), 13 mV (hits), 30 mV (failures), respectively.
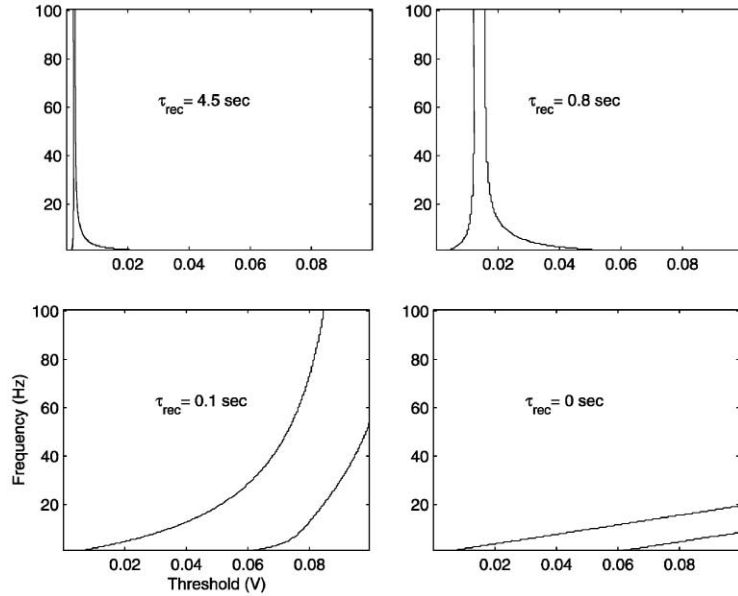
Fig. 2. Regions of detection computed analytically for four different values of τ_{rec} and the same values of other parameters (note that $A_{SE} = 42.5$ pA in all figures). The value of $\tau_{rec} = 0$ s corresponds to the non-depressed (static) synapse. The area of good detection (error less than 60%) is between the curves.

with

$$V_{signal} = M\left[\frac{\tau_m(1 - e^{-1/f\tau_m})}{\tau_{in}(1 - e^{-1/f\tau_{in}})}\right]^{\tau_m/(\tau_{in} - \tau_m)} R_{in} I^{peak} \tag{5}$$

which is obtained by direct integration of Eq. (1).[3] Here, $I^{peak} = A_{SE}U_{SE}(1 - e^{-1/f\tau_{rec}})$ $[1 - (1 - U_{SE})e^{-1/f\tau_{rec}}]^{-1}$ represents the averaged stationary EPSC amplitude of a single synapse [13]. The analytically computed error is presented in Fig. 1(A) (bottom) for dynamic as well as static case.

Both, numerical and analytical phase diagrams, show that there are apparent differences between areas of detection for dynamic and static synapse. To examine how coincidence detection depends on the degree of depression, we have varied τ_{rec}. Fig. 2 illustrates that τ_{rec} strongly affects shape of the (analytical) curves bounding the region of good detection. It can be noticed that for any $\tau_{rec} > 0$, there exists a threshold at which good detection occurs over a large range of frequencies. For increasing τ_{rec} this threshold moves to smaller values that are determined by $\lim_{f \to \infty} V_{noise} = \{(N - M)\tau_{in}\}(\tau_{rec})^{-1}R_{in}A_{SE}$. In Fig. 3 we show the frequency interval

---

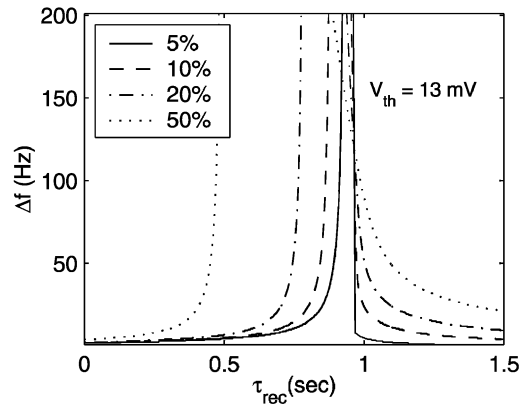[3] The derivation of Eq. (5) is not straightforward and will be published elsewhere.

Fig. 3. The frequency window of detection (Δf) as a function of the degree of depression, i.e. τ_{rec}. Figure shows analytically computed Δf for the fixed threshold of $V_{th} = 13$ mV and different percentages (5%, 10%, 20% and 50%) of coincident spike trains.

for detection (Δf) as a function of τ_{rec} for fixed $V_{th} = 13$ mV and different percentages of coincident spike trains. For each percentage it appears that there is a range of τ_{rec} allowing a large Δf. This range tends to decrease with decreasing percentage of coincident spikes.

4. Discussion

In this study we have analyzed whether a neuron receiving the massive Poissonian spike trains is able to distinguish the coincident spikes from a noisy background. We have shown that short-term depression can have a considerable influence on coincidence detection. In [10] it has been reported that static (non-depressed) synapses are incapable of coincidence detection whereas dynamic (depressed) synapses are. However, these results depend very much on the parameter settings such as the input frequency, the number of coincident spikes, the synaptic strength and the threshold value. Instead, we have shown that for any frequency one can tune the parameters such that both dynamic and static synapses perform equally well. The main difference is that for fixed realistic threshold the frequency-range of detection appears to be larger for the dynamic case. This is consistent with the recent results showing that dynamic synapses can detect relative rate changes over a large frequency range [1]. The above results also stand for the HH neuron for which numerical simulations show the improved coincidence detection with dynamic synapses [9].

References

[1] L.F. Abbott, J.A. Varela, K. Sen, S.B. Nelson, Science 275 (1997) 220.

 [2] W. Bialek, F. Rieke, R.R.D van Steveninck, D. Warland, Science 252 (1991) 1854.
 [3] R.C. Decharms, M.M. Merzenich, Nature 381 (1996) 610.
 [4] L. Dobrunz, C. Stevens, Neuron 18 (1997) 995.
 [5] A. Hodgkin, A. Huxley, J. Physiol. 117 (1952) 500.
 [6] Ch. Koch, Biophysics of Computation: Information Processing in Single Neurons, Oxford University Press, New York, 1999.
 [7] H. Markram, M. Tsodyks, Nature 382 (1996) 807.
 [8] H. Markram, Y. Wang, M. Tsodyks, Proc. Natl. Acad. Sci. USA 45 (1998) 5323.
 [9] L. Pantic, J.J. Torres, H.J. Kappen, unpublished.
[10] W. Senn, I. Segev, M. Tsodyks, Neural Comput. 10 (1998) 815.
[11] C. Stevens, Y. Wang, Neuron 14 (1995) 795.
[12] M. Stopfer, S. Bhagavan, B.H. Smith, G. Laurent, Nature 390 (1997) 70.
[13] M. Tsodyks, H. Markram, Proc. Natl. Acad. Sci. USA 94 (1997) 719.
[14] H. Tuckwell, Introduction to Theoretical Neurobiology I, II, Cambridge University Press, Cambridge, 1988.
[15] M. Wehr, G. Laurent, Nature 384 (1996) 162.

Lovorka Pantic

Hilbert J. Kappen

Joaquin J. Torres